

## THE OPTICAL PROPERTIES OF BRAGG FIBER WITH A FIBER CORE OF 2-DIMENSION ELLIPTICAL-HOLE PHOTONIC CRYSTAL STRUCTURE

**J.-J. Wu**

Department of Electrical Engineering  
Chung Hua University  
Hsinchu, Taiwan 30012, Republic of China

**D. Chen**

Institute of Information Optics  
Zhejiang Normal University  
Jinhua 321004, China,

**K.-L. Liao, T.-J. Yang, and W. L. Ouyang**

Department of Electrical Engineering  
Chung Hua University  
Hsinchu, Taiwan 30012, Republic of China

**Abstract**—The optical properties of birefringent Bragg fiber with a fiber core of 2-dimension (2D) elliptical-hole photonic crystal structure has been studied. Elliptical air holes are introduced into the fiber core to form a normal 2D photonic crystal structure with a hole pitch (center-to-center distance between the air holes) much smaller than the operation wavelength of the Bragg fiber. The elliptical-hole photonic crystal structure acts as an anisotropic medium with different effective indices for transmission light of different polarization, which inevitably results in high birefringence (up to the order of magnitude of 0.01) of the Bragg fiber. The proposed Bragg fiber possesses different band-gaps for differently polarized mode. Besides the periodic alternating layers of high/low refractive indices, the bandwidth of the band-gap is also dependent on the effective index of the fiber core, which can be controlled by the area of the elliptical air holes.

## 1. INTRODUCTION

Photonic crystal fibers (PCFs) [1–4] which also include Bragg fibers [5–8] have attracted increasing interest over the past decade because of their unique property, such as high birefringence, high nonlinearity, endless single-mode operation, single-polarization single-mode operation, and tailorable chromatic dispersion. Highly birefringent PCFs are one kind of extremely important PCFs which have promising applications in e.g., fiber sensors [9], fiber lasers [10, 11], and fiber filters [12]. So far, various highly birefringent PCFs have been proposed [13–17]. Meanwhile, Bragg fibers have recently received much attention for their interesting dispersion and modal properties and for advances in fabrication techniques [18]. However, so far there is no report about birefringent Bragg fibers. As the birefringent Bragg fiber is based on band gap effect; it will be more suitable for bending operation with lower loss. Thus, a combination of Bragg fiber with birefringence is a good trying for the design of novel fibers.

In this paper, we propose a highly birefringent Bragg fiber with a fiber core of 2-dimension elliptical-hole photonic crystal (2D-EH-PhC) structure surrounded by a multilayer cladding with the suitable designed alternating layers of high/low refractive indices. High birefringence (up to the order of magnitude of 0.01) has been achieved and other characteristics of the proposed Bragg fiber have also been investigated.

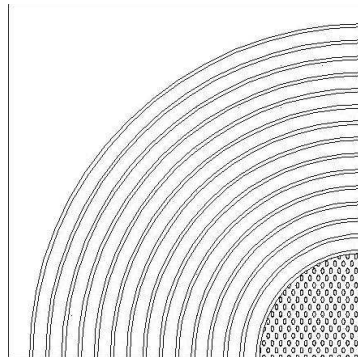


**Figure 1.** Cross section of the proposed Bragg fiber.

## 2. SIMULATION RESULTS AND ANALYSIS

Figure 1 shows a quarter of the cross section of the proposed Bragg fiber with a fiber core of 2D-EH-PhC structure. In the fiber core, the hole pitch  $\Gamma$  (the center-to-center distance between the two adjacent air holes) is 200 nm, which is much smaller than the operating wavelength of the Bragg fibers in this paper. The elliptical air holes are characterized by the normalized area  $S = \pi ab/\Gamma^2$  and ellipticity  $\eta = b/a$ , where  $a, b$  are the radius in  $x$  and  $y$  directions, respectively. The fiber core is encompassed by fifty periodic structures of alternating layers of high and low refractive indices in the fiber cladding. The thickness of the periodic structure formed by one high and one low refractive index layer is  $\Lambda = 387.5$  nm. In this paper, we choose high/low refractive index of 4.6/1.6, with thicknesses of  $d_1 = 0.2176\Lambda$  and  $d_2 = 0.7824\Lambda$  (forming a quarter wavelength waveguide stack for the wavelength within the optical fiber communication window) [19]. The refractive index of the fiber core is set to be 1.45 (considering the silica materials). A full-vector finite-element method (FEM) and anisotropic perfectly matched layers [20] are employed to simulate the guided modes of the proposed Bragg fibers. The calculated results are expressed in terms of the normalized frequency  $\nu = \Lambda/\lambda$ , where  $\lambda$  is the operation wavelength in free space. The phase-index birefringence (PIB) is defined as [21]

$$\Delta n = n_y - n_x \quad (1)$$

where  $n_i$  ( $i = x, y$ ) is the phase modal index.

To understand the characteristics of the Bragg fiber, band structure of the planar dielectric mirror which consists of suitable designed alternating layers of high and low refractive indices with the same parameters as those of the periodic structures of the Bragg fiber mentioned above is shown in Fig. 2. The surface-parallel wave-vector component  $\beta$  and the frequency  $\omega$  are expressed in the unit of  $2\pi c/\Lambda$  and  $2\pi/\Lambda$ , respectively. The heavy gray regions correspond to the situations where light can propagate in the planar dielectric mirror. Hence, for the Bragg fiber with a fiber cladding of the periodic structures, guided modes appear in the white regions in Fig. 2 which are so called band gap regions. The dashed curve represents the light line ( $\omega = c\beta$ ). The solid curve and red dotted curve in Fig. 2 show the dispersion characteristics of  $x$ - and  $y$ -polarized modes for the Bragg fiber with 15 periodic two-layer structures and a fiber core of 2D-EH-PhC structure, respectively. The gap between the two curves indicates the high birefringence of the proposed Bragg fiber.

It is well known that the Bragg fiber with a hollow fiber core (or filled with uniform media) will not be birefringent because of the

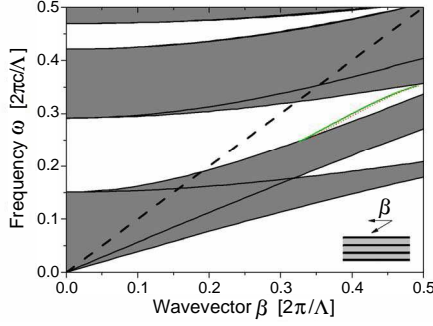


**Figure 2.** Band structure of the planar dielectric mirror and dispersion property for  $y$ -polarized (dotted curve) and  $x$ -polarized (solid curve) modes of the Bragg fiber.

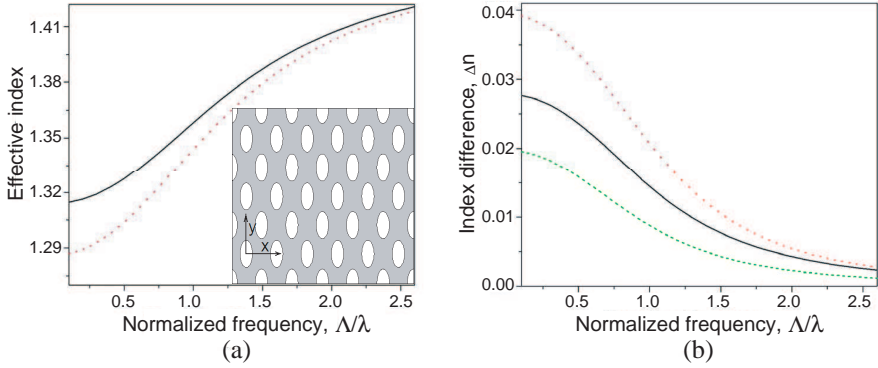


**Figure 3.** (a) Effective index of the 2D-EH-PhC structure for the  $y$ -polarized (solid curve) and  $x$ -polarized (dotted curve) light waves (propagating in the  $z$  direction). (b) Effective index difference of the 2D-EH-PhC for the  $y$ -polarized and  $x$ -polarized light waves. Inset of (a) shows the cross section of the array of elliptical-hole in fused silica.

symmetry. The fiber core of 2D-EH-PhC structure results in the high birefringence. To understand the birefringence induced by elliptical air holes in the fiber, the effective indices of the 2D-EH-PhC material should be investigated carefully. The parameters of the 2D-EH-PhC structure considered here are  $\eta = 2$  and  $S = 0.2$ , as illustrated in the inset of Fig. 3(a). The refractive index of the fused silica is set to be 1.45. A plane-wave expansion method [22] is used to calculate the effective indices for the wave propagation along the  $z$  direction in the

photonic crystal material, and the results are shown as a function of the normalized frequency  $\nu = \Lambda/\lambda$  in Fig. 3(a), where the solid and dotted curves represent the effective indices for the  $y$ - and  $x$ -polarized light waves, respectively. Large difference between the effective indices for differently polarized light waves is observed. Inset of Fig. 3(a) shows the cross section of the array of elliptical-hole in fused silica. Fig. 3(b) shows the index differences when the normalized areas of the elliptical air holes are 0.1 (short dashed curve), 0.2 (solid curve) and 0.3 (dotted curve), respectively. For the photonic crystal material with a normalized area of 0.2, the birefringence reaches its maximum of about 0.0277 as the normalized frequency approaches zero (namely,  $\Lambda$  tends to zero for a given wavelength). This indicates the photonic crystal material can act as an (dispersive) anisotropic medium.

A full-vector finite-element method is employed to analyze the whole guided wave structure. Figure 4(a) shows the birefringence of the proposed Bragg fibers when the ellipticity of the elliptical air holes is 2 and the normalized areas of the elliptical air holes are 0.1 (dashed curve), 0.2 (dotted curve) and 0.3 (solid curve), respectively. Fig. 4(b) shows the birefringence of the proposed Bragg fibers when the normalized area of the elliptical air holes is 0.3 and the ellipticities of the elliptical air holes are 1.5 (dashed curve), 2 (solid curve) and 3 (dotted curve), respectively. Note that the different lengths of the curves in Fig. 4 are due to the fact that different Bragg fibers have different band gap regions. To illustrate the typical field patterns of the modes guided in such Bragger fibers, the major components of the electric fields of the  $x$ - and  $y$ -polarized modes at  $\lambda = 1.5 \mu\text{m}$  are plotted

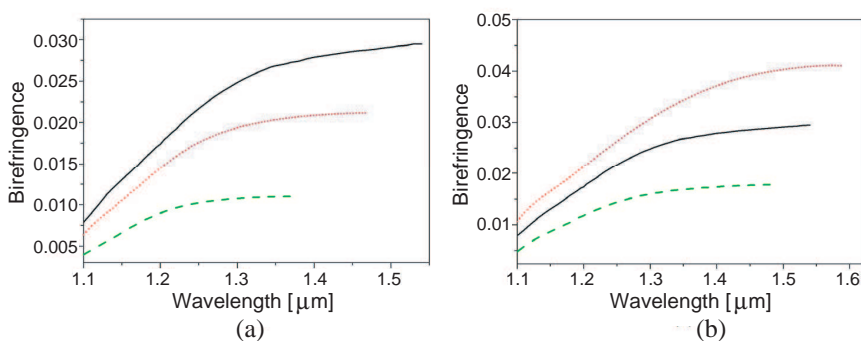


**Figure 4.** (a) Birefringence of the Bragg fibers when the normalized areas are 0.1 (dashed), 0.2 (dotted) and 0.3 (solid), respectively. (b) Birefringence of the Bragg fibers when the ellipticities are 1.5 (dashed), 2 (solid) and 3 (dotted), respectively.

in Figs. 5(a) and 5(b), respectively, where the normalized area of the elliptical holes is  $S = 0.3$  and the ellipticity  $\eta = 2$ .

We also study the confinement loss of the proposed Bragg fibers. Confinement loss can be deduced from the value (imaginary part) of the complex effective index by the expression [16],

$$\frac{40\pi}{\ln(10)\lambda} \text{Im}(n_{eff}) \quad (2)$$

where,  $n_{eff}$  is the complex effective index. Fig. 6 shows the confinement loss of the proposed highly birefringent Bragg fibers when the normalized area of the elliptical air hole 0.1 (dotted curve for  $y$ -polarized mode and dashed curve for  $x$ -polarized mode) and 0.2 (solid curve for  $x$ -polarized mode), respectively. The different effective index of the fiber core for  $x/y$ -polarized light wave results in different loss spectra. Fig. 6 shows the loss for the  $x$ -polarized light wave is much higher than that for the  $y$ -polarized light wave which results in different band gaps for the Bragg fiber with 2D-EH-PhC structure for  $x/y$ -polarized light wave. In addition, when the normalized area of the elliptical air holes increases, the effective index of the fiber core media decreases resulting in lower loss of the Bragg fiber. We have also noted that there are some resonance peaks for the loss curve, which may be due to the optical scattering [23] of the air holes in the fiber core but need to be further investigated.

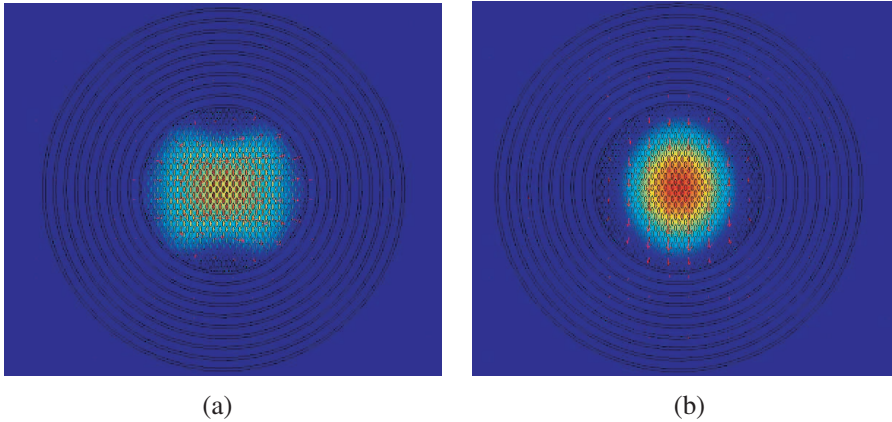


**Figure 5.** Modal profile of the major component of the electric field of the fundamental mode at  $\lambda = 1.5 \mu\text{m}$  for the normalized elliptical-hole area 0.3 and ellipticity 3. (a)  $X$ -polarized mode, (b)  $Y$ -polarized mode.

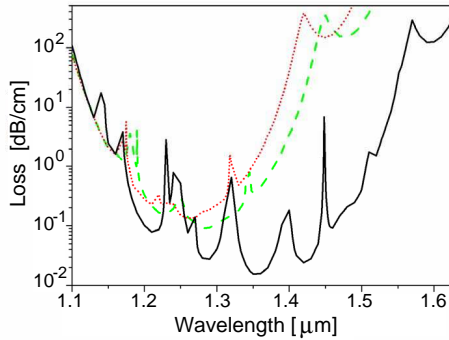


**Figure 6.** Loss of the Bragg fibers. Dotted and dashed lines represent the results for the  $y$ - and  $x$ -polarized modes, respectively, when the normalized elliptical-hole area is 0.1. Solid line is the results for the  $x$ -polarized mode when the normalized elliptical hole area is 0.2.

### 3. CONCLUSION

In conclusion, 2D-EH-PhC structure with a hole pitch much smaller than the operation wavelength is investigated and introduced in the fiber core of the Bragg fiber. High birefringence (up to the order of 0.01) of the Bragg fiber has been achieved since the 2D-EH-PhC structure can act as an anisotropic medium with different effective indices for transmission light of different polarization. Birefringence property of the proposed Bragg fiber has been fully investigated for differently normalized areas or ellipticities of the elliptical air holes in the fiber core. We have also shown the interesting loss characteristics of the proposed Bragg fibers.

### ACKNOWLEDGMENT

This work has been supported by National Science Council (NSC 97-2112-M-216-001). Corresponding email is jjwu@chu.edu.tw.

### REFERENCES

1. Knight, J. C., J. Broeng, T. A. Birks, and P. St. J. Russell, "Photonic band gap guidance in optical fibers," *Science*, Vol. 282, No. 5393, 1476–1478, 1998.

2. Knight, J. C., "Photonic crystal fibres," *Nature*, Vol. 424, 847–851, 2003.
3. Smith, G. M., N. Venkataraman, M. T. Gallagher, D. Müller, J. A. West, N. F. Borrelli, D. C. Allan, and K. W. Koch, "Low-loss hollow-core silica/air photonic bandgap fibre," *Nature*, Vol. 424, 657–659, 2003.
4. Russell, P., "Photonic crystal fibers," *Science*, Vol. 299, 358–362, 2003.
5. Ibanescu, M., Y. Fink, S. Fan, E. L. Thomas, and L. D. Joannopoulos, "An all-dielectric coaxial waveguide," *Science*, Vol. 289, 415–419, 2000.
6. Ouyang, G., Y. Xu, and A. Yariv, "Theoretical study on dispersion compensation in air-core Bragg fibers," *Opt. Express*, Vol. 10, 889–908, 2002.
7. Prokopovich, D. V., A. V. Popov, and A. V. Vinogradov, "Analytical and numerical aspects of Bragg fiber design," *Progress In Electromagnetics Research B*, Vol. 6, 361–379, 2008.
8. Wu, C. J. and S. Gwo, "Calculation of optical properties of an annular dielectric mirror," *Journal of Electromagnetic Waves and Applications*, Vol. 21, No. 6, 821–827, 2007.
9. Frazo, J., M. Baptista, and J. L. Santos, "Temperature-independent strain sensor based on a Hi-Bi photonic crystal fiber Loop Mirror," *IEEE Sens. J.*, Vol. 7, 1453–1455, 2007.
10. Xue, M. and C. Lu, "Self-stabilizing effect of four-wave mixing and its applications on multiwavelength erbium-doped fiber lasers," *IEEE Photon. Technol. Lett.*, Vol. 17, 2541–2543, 2005.
11. Shen, G. F., X. M. Zhang, H. Chi, and X. F. Jin, "Microwave/millimeter-wave generation using multi-wavelength photonic crystal fiber brillouin laser," *Progress In Electromagnetics Research*, PIER 80, 307–320, 2008.
12. Chen, D., "Stable multi-wavelength erbium-doped fiber laser based on a photonic crystal fiber Sagnac loop filter," *Laser Phys. Lett.*, Vol. 4, 437–439, 2007.
13. Steel, M. J. and R. M. Osgood, "Elliptical-hole photonic crystal fibers," *Opt. Lett.*, Vol. 26, 229–231, 2001.
14. Chaudhuri, P. R., V. Paulose, and L. Chao, "Near-elliptic core polarization-maintaining photonic crystal fiber: Modeling birefringence characteristics and realization," *IEEE Photon. Technol. Lett.*, Vol. 16, 1301–1303, 2004.
15. Belardi, W., G. Bouwmans, L. Provino, and M. Douay, "Form-induced birefringence in elliptical hollow photonic crystal fiber

- with large mode area,” *IEEE J. Quantum Electron.*, Vol. 41, 1558–1564, 2005.
16. Chen, D. and L. Shen, “Ultrahigh birefringent photonic crystal fiber with ultralow confinement loss,” *IEEE Photon. Technol. Lett.*, Vol. 19, 185–187, 2007.
  17. Chen, D. and L. Shen, “Highly birefringent elliptical-hole photonic crystal fibers with double defect,” *J. Lightwave Technol.*, Vol. 25, 2700–2705, 2007.
  18. Ouyang, G., Y. Xu, and A. Yariv, “Comparative study of air-core and coaxial Bragg fibers: Single-mode transmission and dispersion characteristics,” *Opt. Express*, Vol. 9, 733–747, 2001.
  19. Johnson, S. G., M. Ibanescu, M. Skorobogatiy, O. Weisberg, T. D. Engeness, M. Soljacic, S. A. Jacobs, J. D. Joannopoulos, and Y. Fink, “Low-loss asymptotically single-mode propagation in large-core omniguide fibers,” *Opt. Express*, Vol. 9, 748–779, 2001.
  20. Saitoh, K. and M. Koshiba, “Full-vectorial imaginary-distance beam propagation method based on a finite element scheme: application to photonic crystal fibers,” *IEEE J. Quantum Electron.*, Vol. 38, 927–933, 2002.
  21. Issa, N. A., M. A. V. Eijkelenborg, and M. Fellet, “Fabrication and study of microstructured optical fibers with elliptical holes,” *Opt. Lett.*, Vol. 29, 1336–1338, 2004.
  22. Meade, R. D., A. M. Rappe, K. D. Brommer, J. D. Joannopoulos, and O. L. Alerhand, “Accurate theoretical analysis of photonic band-gap materials,” *Phys. Rev. B*, Vol. 48, 8434–8437, 1993.
  23. Bertoni, H. L., L. S. Cheo, and T. Tamir, “Frequency-selective reflection and transmission by a periodic dielectric layer,” *IEEE Trans. Antennas Propagat.*, Vol. 37, 78–83, 1989.